

JAN SENTEK, ZENOBIA RŻANEK-BOROCH, MARCIN BRYKAŁA, KRZYSZTOF SCHMIDT-SZAŁOWSKI^{*)}

Warsaw University of Technology

Faculty of Chemistry

ul. Noakowskiego 3, 00-662 Warszawa, Poland

Organo-silicon coating deposition on polyethylene films by pulsed dielectric-barrier discharges

Summary — Organo-silicon coatings deposition from tetraethoxysilane (TEOS) was conducted in pulsed dielectric barrier discharge (PDBD) for packaging polyethylene (PE) films tightening. A laboratory reactor was tested provided with a rotating cylindrical internal electrode bearing the PE film and with a dielectric barrier in the form of a cylindrical glass body was tested. The oxygen permeability of the films was examined after plasma treatment with different gases: He (I), TEOS+He (II), TEOS+He+5 % O₂ (III), TEOS+He+10 % O₂ (IV). For the film surface topography observations, atomic force microscopy (AFM) and scanning electron microscopy (SEM) were used. The coating composition was examined by X-ray photoelectron spectroscopy (XPS) with argon ion sputtering for the determination of individual element contents across the coating. It was found that under PDBD conditions both the treatment in helium plasma and the coating deposition from different TEOS+carrier-gas mixtures reduced the oxygen permeability of PE films.

Key words: thin films, permeation, coating thickness, polymer, pulsed dielectric barrier discharge.

ZASTOSOWANIE IMPULSOWEGO WYŁADOWANIA BARIEROWEGO DO OSADZANIA NA FOLII POLIETYLENOWEJ POWŁOK ZE ZWIĄZKÓW KRZEMU

Streszczenie — Badano plazmowy proces osadzania na powierzchni folii polietylenowej (PE) cienkich powłok uszczelniających złożonych ze związków krzemu. Powłoki osadzano pod ciśnieniem atmosferycznym w impulsowym wyładowaniu barierowym (PDBD) o częstotliwości 400 Hz, w plazmie helowej lub helowo-tlenowej, używając jako substratu tetraetoksyilanu (TEOS). Zastosowany do osadzania powłok laboratoryjny reaktor (rys. 1), składał się z cylindrycznej obrotowej elektrody (na której umieszczano folię) oraz szklanego korpusu z umieszczoną elektrodą wysokonapięciową, pokrywającą tylko niewielką część powierzchni ściany reaktora (przekrój B – B, rys. 1). Dzięki ruchowi obrotowemu elektrody wewnętrznej, umieszczona na jej powierzchni folia przemieszcza się przez strefę wyładowania. Rzeczywisty czas przebywania folii w strefie wyładowania zależy od szerokości elektrody na zewnętrznej ścianie reaktora. Próbki wyjściowej folii oraz próbki folii z osadzonymi w różnych warunkach procesowych powłokami poddawano badaniom za pomocą mikroskopii sił atomowych (AFM) (rys. 6 i 7), skaningowego mikroskopu elektronowego (SEM) (rys. 2 i rys. 5), rentgenowskiego spektroskopu fotoelektronowego (XPS) (rys. 10 i 11) oraz badaniom określającym własności barierowe w odniesieniu do tlenu (rys. 8 i 9). Stwierdzono, że w warunkach PDBD zarówno działanie samej plazmy helowej (I) na folię, jak i osadzanie powłok z mieszanin: TEOS+He (II), TEOS+He+5 % O₂ (III), TEOS+He+10 % O₂ (IV) zmniejszają przenikalność tlenu przez folię. Badania składu powłok metodą XPS (rys. 10 i 11) pokazują, że w ich warstwach powierzchniowych znajduje się SiO₂. Świadczy o tym stosunek atomowy tlenu do krzemu (O/Si ≥ 2). W głębszych warstwach powłoki stosunek tlenu do krzemu zbliża się do jedności.

Słowa kluczowe: cienkie powłoki, przenikalność, polimer, grubość powłoki, impulsowe wyładowanie barierowe.

During the last decade, the atmospheric-plasma techniques have been drawing growing attention as a perspective solution for the commercial processes of surface treatment including thin coatings deposition, etching, cleaning, *etc.* The plasma processes conducted at (or near) the atmospheric pressure are considered as attrac-

tive for both economic and technological reasons compared to traditional physical or chemical processes of surface treatment at lowered pressures. DC corona discharge at atmospheric pressure was the most often used over the last few decades for surface treatment of different materials including polymers, despite the inhomogeneous nature of this discharges [1]. Nevertheless, other plasma techniques such as microwave, DC arc-jet

^{*)} Author for correspondence; e-mail: kss@ch.pw.edu.pl

with extended plasma stream, and dielectric-barrier glow discharge have been also studied for making these processes more efficient. These methods are capital cost saving owing to the inexpensive equipment. On the other hand, however, the productivities of the processes may be lower than those of physical deposition, especially when substrates of large area are treated [2–5].

The plasma techniques are often used for the improvement of packaging materials being the most effective method for producing ultra-thin coatings which seal those materials for better protection of food, cosmetics, and pharmaceuticals and protect them against to the penetration of atmospheric agents. Nowadays, a growing demand is observed for clear barriers against water vapor and oxygen permeability of packaging films. It was found that the most often used silicon oxide (SiO_x) coatings provide superior barrier performance with respect to all plastic-composite materials, besides reducing environmental influence, as they are recyclable [4].

A number of experimental studies have been carried out on both the process parameters and the kind of precursor effects on the barrier properties of the coatings. Their tightness with respect to gases, organic vapors, and water vapor was of particular interest. In the opinion of numerous authors, plasma enhanced chemical vapor deposition (PE-CVD) may be the most suitable technique for thin SiO_x films production with respect to evaporation and sputtering [2–6]. Recently, continuing these investigations of PE-CVD, a number of studies was performed with the use of dielectric barrier discharge (DBD) at atmospheric pressure. Use of pulsed DBD (PDBD) is one of the new ideas in this field [7–11]. The roles played by the vessel configuration and the shape of the plasma zone have been found essential for the PDBD process parameters and their stability during the deposition.

Organic compounds of silicon, *e.g.* tetraethoxysilane (TEOS), tetramethoxysilane (TMOS), hexamethyldisiloxane (HMDSO) and some others, are known as advantageous starting materials for PE-CVD of thin SiO_x coatings. However, because of the complex structure of these compounds, their chemical transformations in plasma are frequently not complete, and thus, the coatings deposited from TEOS, TMOS, HMDSO often contain, besides the SiO_x structure, some “organic” fragments [$\text{Si}(\text{CH}_3)_n$, Si-C , Si-CO , *etc.*]. Such residues affect the quality of the coatings by changing their chemical and mechanical properties, density and adhesion to the substrate. As known, oxygen and other oxidants (*e.g.* N_2O) strongly influence the process of the coating deposition. Oxygen and oxygen containing species (radicals and ion radicals) take part in the reactions proceeding in the plasma zone. This results in an acceleration of the gas reactions, as well as the transformation of the solid organo-silicon product deposited on the substrate surface. The coatings, when produced in the presence of oxygen contain generally more distinct O-Si-O structures and a lower content of organic residues [9, 12–14].

With the aim of reducing of the oxygen permeability of packaging polyethylene films, the study of plasma enhanced organo-silicon thin coating deposition was undertaken with the use of pulsed dielectric-barrier discharges.

EXPERIMENTAL

Materials

The following materials were used in this work:

— polyethylene (PE) packaging film 19–20 μm thick, which cross-section is presented in Figure 1 (60 % of low-density PE and 40 % of crosslinking PE, delivered by PAKPOL, Białystok),

— tetraethoxysilane (TEOS, 98 % purity, supplied by Merck-Schuchardt),

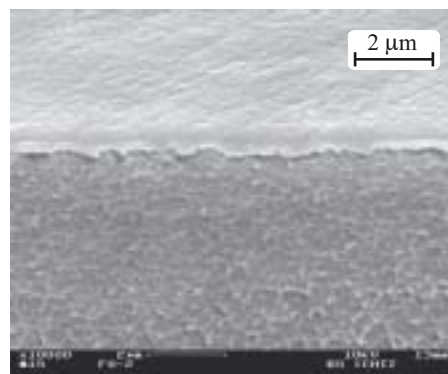


Fig. 1. Cross-section of the polyethylene film ($\times 10\,000$)

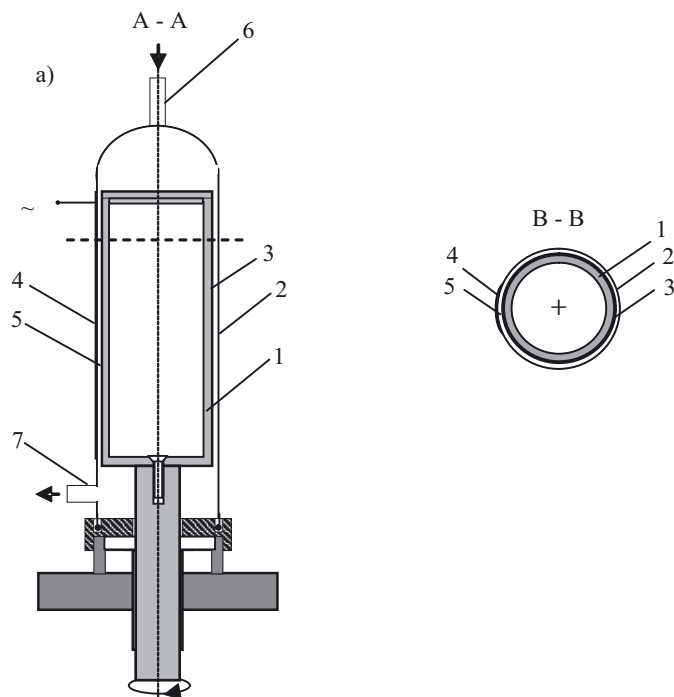


Fig. 2. Scheme of the reactor: a) vertical section A-A; b) horizontal section B-B; 1 — rotating electrode, 2 — glass body, 3 — PE film, 4 — HV electrode, 5 — discharge gap (1.5 mm), 6, 7 — inlet and outlet pipes, respectively

- helium 5.0 (Multax),
- oxygen 5.0 (Multax).

A laboratory reactor developed earlier [10, 11] and used for the present experiment is provided with a rotating cylindrical internal electrode shown in Figure 2 (163 mm long and 65 mm in diameter). It should be mentioned that DBD reactors with rotating electrodes were developed also by other authors [15, 16], however, in different arrangements. The cylindrical glass body of the reactor plays the role of a dielectric barrier and a strip of metal sheet or wire mesh (15 mm wide) attached to the external surface of the glass parallel to the axis is used as a high voltage electrode. The gap distance between the film attached to the rotating electrode surface and the internal surface of the glass body is about 1.5 mm. The PDBD zone is located in the part of the gap near the metal strip which is the external electrode. A sample of the examined polymer film covers the entire surface of the rotating electrode and moves with it through the discharge zone with a constant velocity. The real time of the discharge treating may be controlled by changing the external electrode width, as well as the overall discharge duration.

The reactor is operated at ambient temperature and powered by a pulsed current circuit, composed of an autotransformer for voltage control, high voltage (HV) transformer, HV resistor, Blumlein line, and spark gap. It can generate the voltage pulses of about 60 ns duration up to 15 kV. The pulse frequency may be changed in the range of 100–600 Hz. The voltage and current are recorded by the Tektronix TDS 3032 oscilloscope with probes P 6015A and TCP 202. The main parameters of the discharge were computed as follows:

Instantaneous power (P) during the discharge pulse:

$$P = U(t) \cdot I(t) \quad (1)$$

where: U — voltage, I — current, t — time.

Actual energy (E) released by a single pulse:

$$E = \int_{\tau_1}^{\tau_2} U(t) \cdot I(t) dt \quad (2)$$

where: τ_1 , τ_2 — times at start and finish of the single pulse, respectively.

Charge (Q) transferred by a single pulse:

$$Q = \int_{\tau_1}^{\tau_2} I(t) dt \quad (3)$$

Experiment run

The scheme of the experimental apparatus is shown in Figure 3. TEOS used as a precursor was a component of the feed gas mixtures with helium or with helium and oxygen. The process was carried out at atmospheric pressure with constant helium flow rate of 10 Nm³/h. The TEOS vapor was added to the gas stream at the rate of 0.6 mmol/h by evaporation of the liquid at constant temperature. The TEOS concentration (0.13 mol % in

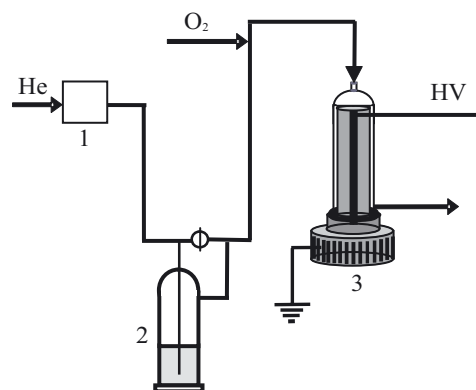


Fig. 3. Scheme of the experimental equipment: 1 — flow controller, 2 — TEOS saturator, 3 — PDBD reactor

mixture with helium) was measured by weighing liquid TEOS in the bubbler. In two series of experiments, oxygen was added to the mixture He+TEOS in an amount of 5 or 10 % in relation to the helium content. The following gas compositions have been tested:

- pure He (I),
- TEOS+He (II),
- TEOS+He+5 % of O₂ (III),
- TEOS+He+10 % of O₂ (IV).

The residence time of gas mixtures in the discharge gap was about 18 s and the durations of the actual plasma action ranged from 2.2 to 44 s. In all experiments, pulsed discharges of frequency of 400 Hz were used. Starting the experiment, the selected feed gas was passed through the reactor. After the discharge parameters had been set, the drive of the inner electrode rotation was started. From this moment, the polymer film moved with the rotating electrode through the discharge zone with a constant velocity (3 s for one turn).

Two kinds of the HV external electrodes were used:

- a strip of aluminum sheet 0.05 mm thick and 15 mm wide,
- a strip of stainless steel wire mesh 325 of the same width.

Coating characterization

The permeability of oxygen was determined at 30 °C from the measurement of the oxygen diffusion rate through the examined film using an interferometer for the gas analysis. The residue permeability (R) is computed from the formula:

$$R = \frac{P_i}{P_0} \cdot 100 \% \quad (4)$$

where: P_i — permeability after treatment [cm³ O₂/(cm² · s · cm Hg)], P_0 — permeability of the virgin film equal to 60 · 10⁻¹⁰ cm³ O₂/(cm² · s · cm Hg).

The mass of coating was measured gravimetrically for long duration of the plasma action and the deposition rates were calculated based on these measurements.

The surface topography was studied using atomic force microscope (AFM) NanoScope IIIA Digital Instruments Veeco Group.

The coating elemental composition was determined by X-ray photoelectron spectroscopy (XPS) using a VG Scientific ESCALAB-210 spectrometer with an Al $K\alpha$ X-ray source (1486.6 eV). The changes in contents of individual elements across the layers could be observed due to the coating sputtering with an argon ion gun AG-21.

The scanning electron microscope (SEM) images of the films were obtained with the use of the microscope Zeiss DSM 942.

RESULTS AND DISCUSSION

Discharge characteristics

Series of measurements were performed to examine the course of individual discharge pulses. As can be seen from Table 1 and Figure 4, the shapes of current and power pulses were similar for both HV electrodes applied. With the use of the aluminum sheet, however, the energy released in the single pulse was about 1.7 times higher than for wire mesh one.

Table 1. Pulse characteristics in helium gas with different HV electrodes: aluminum sheet or wire mesh; frequency 400 Hz

HV electrode	Pulse duration, ns	Energy released, mJ	Charge transferred, μC
aluminum	63	79	6.5
wire mesh	63	45	6.3

Scanning electron microscopy

Figure 5 presents the SEM image of the coating deposited on the PE substrate. The coating deposited from the feed gas containing 5 % of O_2 (III) was of exceptionally high thickness (190 nm) owing to the prolonged

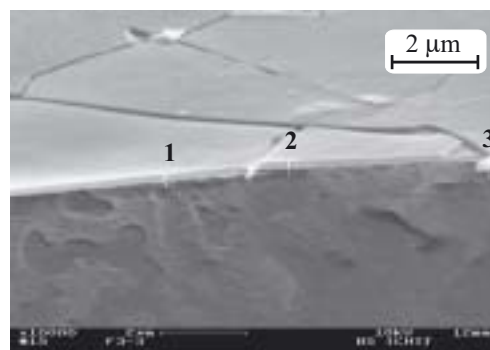


Fig. 5. Cross-section of the PE film with the coating deposited from the mixture TEOS+He+5 % of O_2 for 110 s ($\times 10\,000$, view at the angle of 75°), the thickness at denoted points: 1 — 190 nm, 2 — 196.4 nm, 3 — 183.1 nm

deposition time of up to 110 s. The net of the micro-crushes which is clearly seen, was probably one of the reasons of the increased permeability of the thicker coatings.

Atomic force spectroscopy

Table 2. Results of AFM study of the surface topography with different HV electrodes and various feed gas mixtures

HV electrode	Gas mixture	Treatment time, s	R_q^a , nm	Z^b , nm
aluminum	I	2.2	6.155	55.91
	II		3.257	27.53
	III		2.397	20.87
Wire mesh	I	8.8	3.611	29.59
	II		4.068	35.42
	III		4.766	36.36
Virgin PE			0.805	7.82

a) R_q — RMS average of height deviation from mean data plane.

b) Z — maximal vertical distance between the highest and lowest data points.

The surface topography investigations showed that the preliminary roughness of the unmodified PE surface

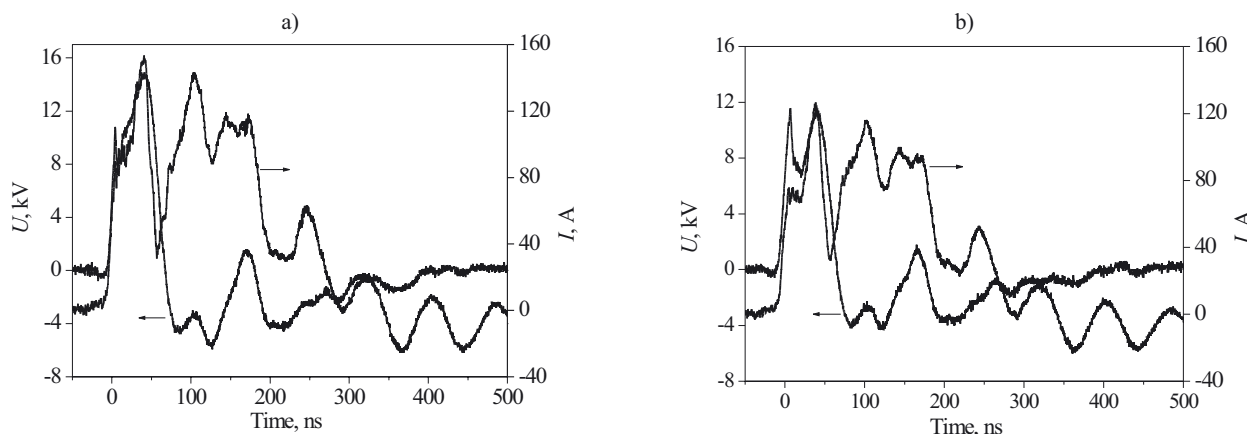


Fig. 4. Pulse voltage and current courses: a) HV electrode of aluminum sheet, b) HV electrode of wire mesh

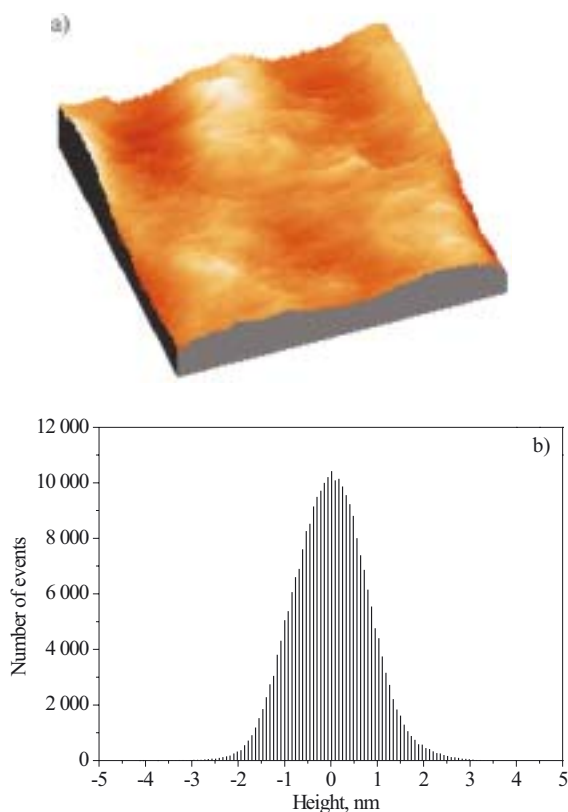


Fig. 6. AFM image of the virgin PE film: a) 3D image, b) height deviation distribution (referred to the mean plane)

increased owing to plasma treatment in all of the gases tested: (He, TEOS+He and TEOS+He+5 % of O₂) (Table 2). Examples of the surface topography of PE films unmodified and plasma-treated are given in Figures 6 and 7. The effect of plasma treatment on polymer surface roughness was observed earlier in a number of studies *e.g.* [1, 17].

Deposition rate

The deposition rate was assessed by gravimetric measurements for the deposition time of 110 s. Both kinds of HV electrodes were tested. It can be seen from the results given in Table 3, that the maximum deposition rate [$1.8 \cdot 10^{-5}$ g/(cm² · min)] was achieved using aluminum electrode and the feed gas mixture III.

Table 3. Deposition rates for different HV electrodes during deposition time 110 s on the film area 326 cm²

Gas mixture	HV electrode	aluminum		wire mesh	
		coating mass, g	deposition rate g/(cm ² · min)	coating mass, g	deposition rate g/(cm ² · min)
I		0.0086	$1.4 \cdot 10^{-5}$	0.0025	$0.4 \cdot 10^{-5}$
III		0.0106	$1.8 \cdot 10^{-5}$	0.0059	$1.0 \cdot 10^{-5}$
IV		0.0088	$1.5 \cdot 10^{-5}$	0.0076	$1.3 \cdot 10^{-5}$

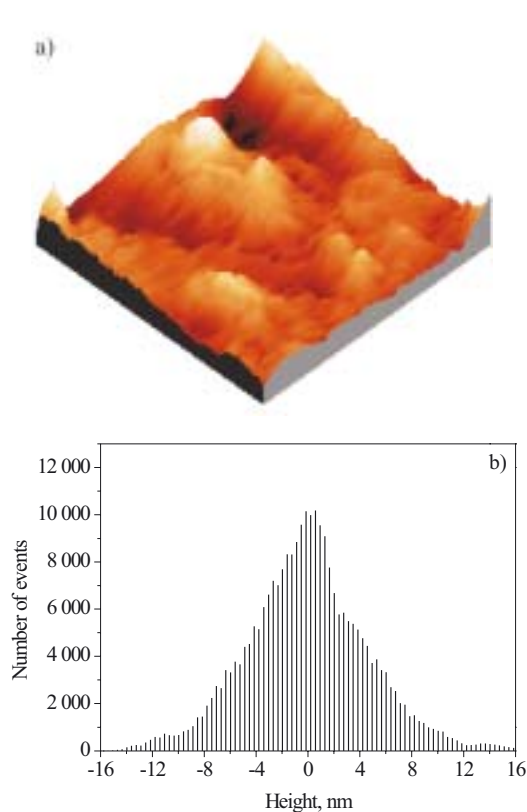


Fig. 7. AFM image of the coating deposited from III gas mixture during 8.8 s using wire mesh electrode: a) 3D image, b) height deviation distribution (referred to the mean plane)

Permeability reduction

The reduction of PE permeability was studied using feed gases of different compositions and both kinds of HV electrodes. Results of these investigations are presented in Figures 8 and 9. Two interesting effects were observed. One of them was the reduction of PE permeability by pure helium plasma treatment — *R* attained the level of 50–60 % referred to the unmodified film. The other one was an influence of the oxygen concentration on the permeability reduction. Generally, the best effects were observed for the feed (III): minimum *R* for aluminum electrode was about 35 %, and for wire mesh electrode was lower than 30 %. With higher oxygen concentration [feed gas (IV)] *R* values were higher. On the other hand, the treatment time was found to be an essential parameter of the experiment. It is characteristic that for the most efficient feed (III), the *R* values reached their minima in the region of shorter treatment times: 2.2–8.8 s. When the treatment was prolonged (up to 22 or 44 s), the residual permeability increased.

There may be different circumstances influencing the coating permeability. As known, a high reduction of permeability may be reached at the moment when the entire surface of the substrate is covered by the tight coating. After that, however, when the coating continues growing under plasma action, its adherence to the substrate

surface becomes weaker, and therefore, the local micro-cracks may occur. It seems probable that the weakening bond and formation of micro-cracks between the thick deposited layer and the surface of the film were the main reason for increased permeability. Those micro-cracks could be easily noticed in SEM image of the thick coating in Fig. 5 (the maximum thickness was about 190 nm). There may be, however, another reason of the increased

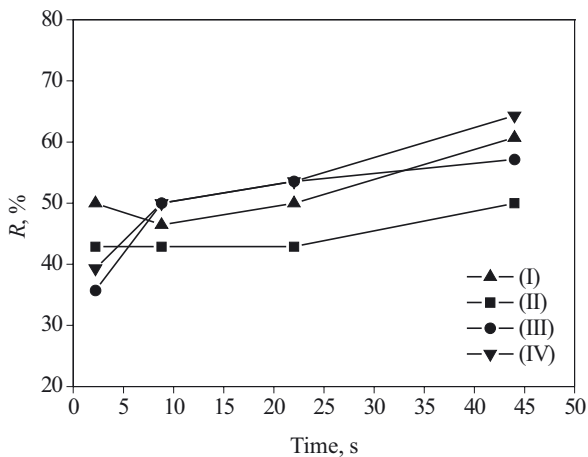


Fig. 8. Residual permeability R of PE films; plasma treated using aluminum electrode, during 2.2 to 44 s in different gases (I–IV)

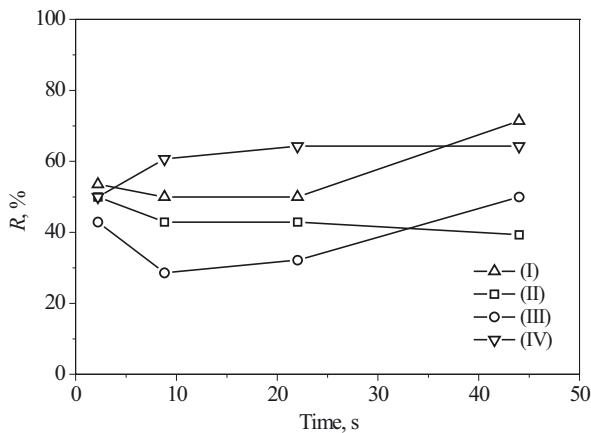


Fig. 9. Residual permeability R of PE films; plasma treated using wire mesh electrode, during 2.2 to 44 s in different gases (I–IV)

permeability observed during the longer treatment. As known, in most cases dielectric barrier discharge is not uniform, as is composed of a number of tiny micro-discharges. It is possible that some instantaneous stronger micro-discharges randomly formed in the plasma zone may locally damage the deposited coating producing pinholes [18]. A rising number of the pinholes during the prolonged treatment time may be the reason of decreasing barrier effect of the coating. This problem will be discussed later.

X-ray photoelectron spectroscopy

Data analysis of the XPS spectra was performed using the ECLIPSE data system software. The binding energy (BE) scale was calibrated by a C1s peak at 285.0 eV. Surface sputtering was carried out using an argon ion gun AG-2, with the ion beam parameters: 3 kV, 10 mA. Seven measurements performed during the sputtering time of 60 min allowed to assess the elemental composition of the coating as well as the dominating silicon forms at different depths across the coating (hydrogen is not determined by this measurement). The composition of the coating deposited from the feed gas (III) (Figures 10 and 11) is characterized by a large share of carbon (about 80%), over the examined coatings depth. This result could be assigned to the organic residues (from the precursor) and/or to the penetration of the substrate structure fragments into the coating, an effect of the plasma action. Similar effects were observed during organo-silicon coating deposition on polycarbonate substrate by PDBD, however with much lower carbon content in the coating internal part [19]. The conclusion regarding the essential effect of carbon compound penetration from the PE surface may be confirmed by

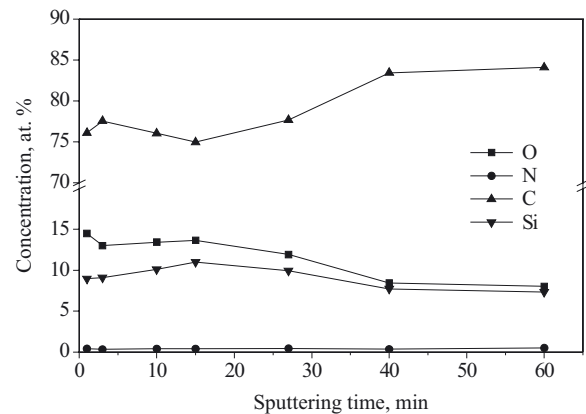


Fig. 10. Element concentrations across the coating deposited from the feed gas III during 22 s, using wire mesh electrode

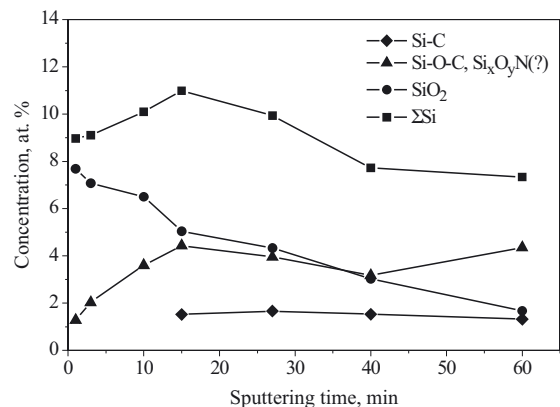


Fig. 11. Different forms of silicon in the coating deposited from the feed gas III during 22 s, using wire mesh electrode

comparison of these values with those obtained for a similar coating deposited from TEOS, on a silicon surface. Using DBD discharge of 1300 Hz frequency and the feed gas composition of TEOS+Ar+O₂ a 100 nm thick coating was deposited at temp. 212 °C on Si monocrystal substrate [20]. Only in the surface layer of this coating, the carbon concentration was higher than 20 at. %, being much lower in deeper layers. In this case, there was no other carbon source than the precursor molecules.

In Fig. 11, various forms of silicon are shown as recorded in the XPS spectra, mainly SiC, SiOC, and SiO₂. The content of Si was the highest near the coating surface (with the O/Si atomic ratio nearly 2), however, in the deeper layers, the O/Si atomic ratio decreased to nearly 1.

Discussion

It was shown that the PDBD plasma treatment of PE films with all the examined feed gases (I—IV) influence their permeability and the silicon compound coatings may be effectively deposited from the gas mixtures II—IV. In accordance with the earlier results [9, 12] it was observed that the presence of oxygen strongly affected the coating deposition. At experiment conditions, the deposition rate increased with increasing oxygen concentrations up to 5 %. Taking into account the known mechanism of the thin coating formation from TEOS+O₂ mixtures, it can be expected that as a result of the reaction of TEOS with oxygen, diethoxysilane [(EtO)₂Si=O] is produced as the main intermediate reactant for the solid deposit formation owing to the plasma polymerization. At the same time, the growing layer of organo-silicon deposit is modified by the action of energized species including the active forms of oxygen and other radicals [12]. Only in cases when this process is completed, the SiO_x is the sole inorganic product in the coating. In the present experiment, however, the coating formation was interrupted at an early stage of transformation when the share of organic structures was dominating (see XPS studies — Figs. 10 and 11). Moreover, the penetration of the PE structure fragments from the substrate surface under plasma action was a source of additional amounts of carbon containing components. Both effects should be considered as probable reasons of the high carbon and low silicon compound shares in the coatings.

The barrier properties of the coatings are characterized by residue permeability for oxygen of about 30 % or higher. Different circumstances may be responsible for that:

- pinholes and other damages produced by the discharge channels,
- micro-cracks occurring owing to low mechanical strength and weak adhesion to the substrate,
- high porosity of the coating and high roughness (Table 2).

As can be seen from the current course during the pulses (Fig. 4), the discharge is rather of homogeneous character with no traces of stronger individual microdischarge channels being able to produce pinholes. On the other hand, in microscopic images of the coatings only few pinholes or other damages are found. Thus, one can conclude that the first reason is not responsible for the results observed. However, micro-cracks may be a possible reason of high permeability, in the case of thick coatings. This was observed in the image of the coating of maximum thickness (about 190 nm) produced in the actual deposition time of 110 s using the feed gas (III) (Fig. 5). For the thin layers (*e.g.* 10 nm), however, the probability of micro-cracks' formation is rather low. Thus, the third suggestion should be considered as the most probable reason of the residue permeability of the coating, namely the porosity and roughness of the polymer layer deposited on the PE surface. The low conversion of the complex organo-silicon deposit on the surface into a continuous and tight SiO_x structure may facilitate the oxygen diffusion across the coating. On the other hand, because of high roughness of the deposit layer, there may be a great number of the local valleys and micro-caverns making gas penetration possible. One can conclude that such circumstances make the coating barrier function less effective.

It is noteworthy that our earlier studies have revealed that similar results were obtained when the experiments with the PDBD deposition of thin coatings on PE using gas mixtures were carried out with argon (instead of helium) [21]. For example, in the coating deposited from the gas mixture TEOS+Ar+O₂ (5 %), the carbon share was found to be higher than 80 %, and *R* value was at the level of 25 %.

CONCLUSIONS

— Using the pulsed dielectric barrier discharge (PDBD), the coatings of silicon compounds were effectively deposited on PE packaging films with the use of tetraethoxysilane (TEOS) in the following mixtures TEOS+He, TEOS+He+5 % of O₂, and TEOS+He+10 % of O₂, and the reduction of their permeability was observed.

— The PDBD treatment of PE films in pure helium resulted in the reduction of their permeability to 50—60 % of that of the unmodified film.

— The presence of oxygen affected the coating deposition rate and the residual permeability of the PE films. The deposition rate increased with increasing oxygen content up to 5 %. The use of mixture of TEOS+He+5 % of O₂ let reach the level of the residual permeability of 30—35 %.

— The high content of carbon in the coatings resulted from the share of organic structures, which were residues of the precursor (TEOS), and of PE structure fragments from the substrate surface.

— The porosity and roughness of the coatings composed of a complex organo-silicon deposit were the main reasons of the high level of the residual permeability of PDBD treated PE films.

ACKNOWLEDGMENTS

This work was financially supported by the Warsaw University of Technology, Warszawa, Poland.

REFERENCES

1. Żenkiewicz M.: *Polimery* 2008, **53**, 3.
2. Hopfe V., Sheel D. W.: *IEEE Trans. Plasma Sci.* 2007, **35**, 204.
3. Madocks J., Rewhinkle J., Barton L.: *Mater. Sci. Eng.* 2005, **B 119**, 268.
4. Creatore M., Palumbo F., d'Agostino R.: *Pure Appl. Chem.* 2002, **74**, 407.
5. Foest R., Adler F., Sigeneger F., Schmidt M.: *Surf. Coat. Technol.* 2003, **163 — 164C**, 305.
6. Czeremuszkin G., Latreche M., Wertheimer M. R., da Siva Sobrinho A. D.: *Plasmas Polym.* 2001, **6**, 107.
7. Okazaki K., Nozaki T.: *Pure Appl. Chem.* 2002, **74**, 447.
8. Opalińska T., Ulejczyk B., Karpiński L., Schmidt-Szałowski K.: *Pol. J. Chem. Technol.* 2002, **4**, 30.
9. Ulejczyk B., Ekwińska M. A., Opalińska T., Karpiński L., Rymuza Z., Scholz M., Żukowska E., Schmidt-Szałowski K.: *Czech. J. Phys.* 2006, **B 56**, 1383.
10. Sentek J., Krawczyk K., Kuś M., Schmidt-Szałowski K.: *Pol. J. Chem.* 2005, **79**, 1539.
11. Sentek J., Olińska K., Deptuła H.: *Pol. J. Appl. Chem.* 2005, **49**, 153.
12. Wróbel A. M., Walkiewicz-Pietrzykowska A., Wickramanayaka S., Hatanaka Y.: *J. Electrochem. Soc.* 1998, **145**, 2866.
13. Zajickova L., Brusickova V., Kucerova Z., Franclova J., Stahel P., Perina V., Mackova A.: *J. Phys. Chem. Solids* 2007, **68**, 1255.
14. Shujun Yang, Hong Yin: *Plasma Chem. Plasma Process.* 2007, **27**, 23.
15. Vinogradov I. P., Dinkelman A., Lunk A.: *Surf. Coat. Technol.* 2003, **174**, 509.
16. Borcia G., Anderson C. A., Brown N. M. D.: *Appl. Surf. Sci.* 2004, **221**, 203.
17. Foldes E., Toth A., Kalman E., Fekete E., Tomassovsky-Bobak A.: *J. Appl. Polym. Sci.* 2000, **76**, 1529.
18. Da Silva Sobrinho A. S., Czeremuszkin G., Latreche M., Wertheimer M. R.: *Appl. Phys. A* 1999, **68**, 103.
19. Opalińska T., Ulejczyk B., Schmidt-Szałowski K.: *IEEE Trans. Plasma Sci.* 2009, **37**, 934.
20. Schmidt-Szałowski K., Fabianowski W., Rżanek-Boroch Z., Sentek J.: *J. Chem. Vap. Deposition* 1998, **6**, 183.
21. Sentek J., Kuś M., Schmidt-Szałowski K.: *Przem. Chem.* 2006, **85**, 258.

Received 11 XII 2008.